Thin Film Microstructure of a Solution Processable Pyrene-Based Organic Semiconductor

Leah A. Lucas,[†] Dean M. DeLongchamp,*[,‡] Lee J. Richter,[‡] R. Joseph Kline,[‡] Daniel A. Fischer,[‡] Bilal R. Kaafarani,*[,§] and Ghassan E. Jabbour*[,†]

School of Materials and Flexible Display Center, Arizona State University, Tempe, Arizona 85284, Polymers Division, Surface and Microanalysis Science Division, Ceramics Division, National Institute of Standards and Technology, Gaithersburg, Maryland 20899, and Department of Chemistry, American University of Beirut, Beirut, Lebanon

Received September 28, 2007. Revised Manuscript Received February 25, 2008

Semiconducting 6,7,15,16-tetrakis(dodecylthio)quinoxalino[2′,3′:9,10]phenanthro[4,5-*abc*]phenazine (**TQPP-12**) has been synthesized as a candidate solution-processable semiconductor for organic electronics applications. We characterize the microstructure of **TQPP-12** in films using a combination of polarized photon absorption spectroscopies (X-ray, vis, and infrared), X-ray diffraction, and scanning probe techniques. This characterization strategy allowed for the determination of molecular orientation and packing style within thin films of this complex molecule. The **TQPP-12** molecules are arranged within layers, and the aromatic cores are separated from the alkane side chains. Both the core long axes and side chains are highly tilted with respect to surface normal, and the conjugated planes of the core are cofacially packed.

Introduction

Identifying organic semiconductor microstructure and determining how it relates to carrier mobility continues to challenge the development of new materials for organic electronics. Establishing these relationships is a necessary step toward controlling thin film crystallization processes to realize greater carrier mobility and more facile processing methods. The organic semiconductor **TQPP-12** (6,7,15,16-tetrakis(dodecylthio)quinoxalino[2′,3′:9,10]phenanthro[4,5-*abc*]phenazine) (Figure 1a) has been developed as a potential charge transport material for organic electronics applications.[1] Similar charge transport materials having a rigid central aromatic core with flexible chains attached to the core edge have been shown to pack in well-defined columns that form one-dimensional pathways for charge transport because of intermolecular π-orbital overlap.[2,3] It has been suggested that **TQPP-12** exhibits similar packing behavior, but its thin film microstructure has not yet been reported.

Probing the thin film crystal structures of complex organic molecules is challenging because they often form unit cells with complex spatial and orientational arrangements of their chemical moieties. X-ray diffraction (XRD) can be applied to thin films in grazing incidence mode (GIXD), but even this measurement rarely affords sufficient detail to assign positions and orientations to all moieties of a complex molecule, though it has proven powerful for determining the microstructure of completely rigid fused ring systems such as pentacene.[4,5] Developing complete structure models for more complex molecules requires multiple, complementary measurements.

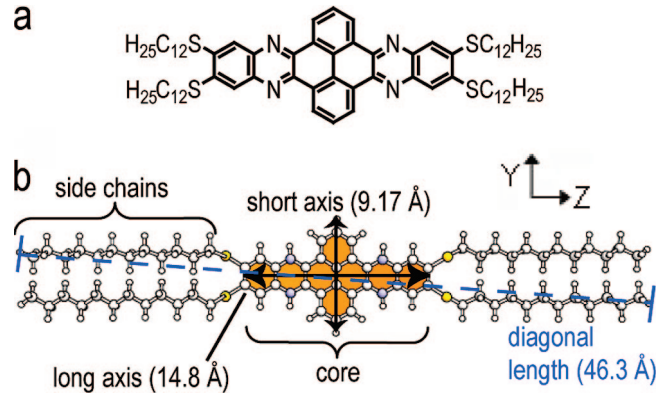

Figure 1. (a) Chemical structure of **TQPP-12**. Axes define transition dipole orientation, which is discussed in the later IR spectroscopy analysis. (b) **TQPP-12** based on semiempirical (AM1) Hamiltonian calculation. Side chains are fully extended from core.

Here we demonstrate a strategy for characterizing the microstructure of **TQPP-12** that complements XRD with polarized photon absorption spectroscopies including polarized infrared (IR) spectroscopy, spectroscopic ellipsometry (SE), and near-edge X-ray absorption fine structure (NEXAFS) spectroscopy. These combined spectroscopies allow for the independent determination of the

* Corresponding author. E-mail: jabbour@asu.edu (G.E.J.); dean.delongchamp@nist.gov (D.M.D.); bilal.kaafarani@aub.edu.lb (B.R.K.).
[†] Arizona State University.
[‡] National Institute of Standards and Technology.
[§] American University of Beirut.

(1) Kaafarani, B. R.; Lucas, L. A.; Wex, B.; Jabbour, G. E. *Tetrahedron Lett.* **2007**, *48*, 5995–5998.
(2) Kumar, S. *Chem. Soc. Rev.* **2006**, *35*, 83–109.
(3) Cornil, J.; Lemaur, V.; Calbert, J.-P.; Brédas, J.-L. *Adv. Mater.* **2002**, *14*, 726–729.
(4) Fritz, S. E.; Martin, S. M.; Frisbie, C. D.; Ward, M. D.; Toney, M. F. *J. Am. Chem. Soc.* **2004**, *126*, 4084–4085.
(5) Mayer, A. C.; Kazimirov, A.; Malliaras, G. G. *Phys. Rev. Lett.* **2006**, *97*, 105503.

10.1021/cm702802w CCC: $40.75
Published on Web 08/28/2008

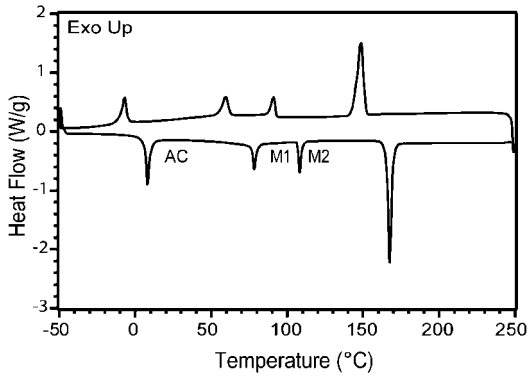

Figure 2. DSC thermogram of **TQPP-12** bulk powder upon second heating/cooling cycle at 10 °C/min. Thin film processing conditions labeled for as-cast film at room temperature (AC), film annealed at 95 °C (M1) and film annealed at 120 °C (M2).

surface-relative orientations of the core long and short axes, the conjugated π-plane, and the side chains. When combined with spacing information from XRD, this information allows us to determine the packing style of this complex molecule.

Experimental Methods

TQPP-12, shown in the Figure 1a, was prepared by a previously reported synthesis.[1] Silicon wafers were first exposed to ultraviolet (UV) ozone treatment for 10 min. Silicon substrates were modified with octyltrichlorosilane (OTS) purchased from Gelest, Inc. from a 2 mmol/L solution in anhydrous hexadecane (Aldrich) for 18 h at 25 °C. (Certain commercial equipment, instruments, or materials are identified in this paper to foster understanding. Such identification does not imply recommendation or endorsement by the National Institute of Standards and Technology, nor does it imply that the materials or equipment identified are necessarily the best available for this purpose.) Thin films of **TQPP-12** were spin coated at 3000 rpm ($3000 \times 2\pi$ rad min^{-1}) from 5 mg mL^{-1} solutions in anhydrous toluene onto the OTS-modified Si substrates in a nitrogen environment. The average **TQPP-12** film thickness was (30 to 35) nm as measured by atomic force microscopy (AFM) and spectroscopic ellipsometry (see below). Bulk differential scanning calorimetry (DSC) measurements were performed on a T.A. Instruments DSC Q1000 from (−50 to 250) °C with a heating rate of 10 °C/min and nitrogen purge. Powder samples were sealed in aluminum pans under a nitrogen environment. **TQPP-12** exhibits multiple phases as shown in Figure 2. To explore these thermal transitions, films were prepared with three distinct thermal histories: (1) as-cast (AC), (2) heated to the first high-temperature phase (M1, $T = 95$ °C), and (3) heated to the second high-temperature phase (M2, $T = 120$ °C). M1 and M2 films were heated to the appropriate temperature for 5 min in a nitrogen environment and then immediately cooled on a stainless steel plate.

XRD. Specular X-ray diffraction spectra were collected in a $\theta-\theta$ configuration on a Scintag diffractometer with a Cu Kα source. All spectra were collected under vacuum (~4.5 Pa). Grazing incidence X-ray diffraction (GIXD) spectra were collected with a Rigaku diffractometer using a Mo Kα_1 beam passing through three pinholes with the entire beam path and sample under vacuum. A two-dimensional 30 cm × 30 cm image plate was used for data acquisition. An incidence angle of 0.1° was used.

AFM. Atomic force microscopy (AFM) was performed with a Dimension 3100 (Veeco) in tapping mode.

Near-Edge X-ray Absorption Fine Structure (NEXAFS) Spectroscopy. NEXAFS spectroscopy was performed at NIST beamline U7A at the National Synchrotron Light Source (NSLS) of Brookhaven National Laboratory. NEXAFS spectra were collected over the carbon K-edge (≈285 eV) at several incident angles with respect to the surface plane (20°, 33°, 44°, 55°, and 80°). NEXAFS spectra were collected in partial electron yield (PEY) mode and a grid bias of −50 V. The incident angle dependent NEXAFS can be used to characterize the orientation of alkane side chains and conjugated plane by the dichroism in the σ^* and π^* resonances, respectively.[6]

Spectroscopic Ellipsometry. Variable angle spectroscopic ellipsometry (VASE) data was collected at 45.0, 32.5, and 20.0° with respect to the surface plane on **TQPP-12** films spun on OTS-modified Si wafers using an M-2000 series ellipsometer (J. A. Woollam Co., Inc.). The VASE data were fit to simple model of a uniaxial dielectric function with variable thickness. To reduce correlations between the fit parameters, identical films were cast on a native oxide (~1.8 nm thickness) and a thermal oxide (~200 nm thickness) substrate, and the two films combined in the analysis.[7]

Polarized IR Spectroscopy. TQPP-12 thin films were prepared on double side polished Si wafers. The sample chamber of a Magna 860 FTIR (Thermo Nicolet) was equipped with a variable angle goniometer used to position the sample at Brewster's angle (16.3°) with respect in the incident IR beam. Both s (electric field vector perpendicular to the plane of incidence) and p (electric field vector in the plane of incidence) polarized transmission spectra were recorded using a wire grid polarizer. The spectra were quantified by a nonlinear least-squares fit to multiple Lorentzian lines. Further experimental details can be found in ref 8. Uncertainties were calculated as an estimated standard deviation from the mean.

Results and Discussion

Our strategy for characterizing the microstructure of **TQPP-12** begins with XRD because diffraction provides a direct signature of regular order, and the layer *d*-spacing along the thin film normal can be compared to molecular dimensions to determine likely molecular orientations. As described in Experimental Methods, thin films of **TQPP-12** on OTS-modified Si substrates were first prepared according to the AC (as-cast), M1 (first phase), and M2 (second phase) thermal histories. Specular XRD patterns of AC and M1 films are shown in Figure 3. Peaks are indexed as marked. Peak positions and widths are provided in the Supporting Information. Notably, the diffraction pattern does not change upon heating to the M1 phase. A similar result was found for the M2 thermal history. Despite the thermal transitions observed by bulk powder DSC, the out-of-plane layer spacing and crystallinity are unaffected by thermal history. In all films, the out-of-plane (00*l*) peak series corresponds to a layer *d*-spacing of 34.3 ± 0.3 Å. The (002) diffraction peak full width at half-maximum (fwhm) can be analyzed by the Scherrer relationship.[9] The derived coherence length of 2π/fwhm ≈ 31 nm corresponds to the film thickness, indicating that

(6) DeLongchamp, D. M.; Lin, E. K.; Fischer, D. A. *Proc. SPIE* **2005**, *5940*, 54–64.
(7) Tammer, M.; Monkman, A. P. *Adv. Mater.* **2002**, *14*, 210–212.
(8) Gurau, M. C.; DeLongchamp, D. M.; Vogel, B. M.; Lin, E. K.; Fischer, D. A.; Sambasivan, S.; Richter, L. J. *Langmuir* **2007**, *23*, 834–842.

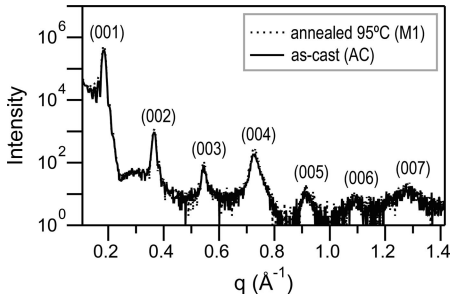

Figure 3. XRD patterns for AC and M1 (annealed at 95 °C) film. Primary peaks are indexed as marked. XRD of M2 film (not shown) produced similar results. Peak position and widths are available in the Supporting Information.

the film is crystalline throughout. The irregular variation in peak intensity, as a function of peak order, indicates a complex structure factor. A single **TQPP-12** molecule with flattened side chains fully extended from the conjugated core would have an estimated diagonal length of 46.3 Å, based on a semiempirical Hamiltonian (AM1) structure calculation[24] as drawn in Figure 1b. The specular XRD layer spacing therefore suggests that parts of the molecule must be substantially tilted within an assumed monomolecular lattice.

AFM studies indicate that the surface morphology, in contrast to the layer structure observed by XRD, does change upon thermal treatment. Figure 4a,b shows AFM micrographs of AC and M1 films, respectively. The M1 thermal history permits the development of well-defined terraces as indicated by the two sharp levels of common *z*-height displayed in the histogram inset of Figure 4b. Size analysis indicates an average lateral dimension of ~275 nm for the M1 thermal history. The AC film, in contrast, has a significantly broader *z*-height distribution (Figure 4a), indicating poorer terrace definition. Size analysis indicates an average lateral dimension of ~100 nm for the AC thermal history. In the height distribution histograms of Figure 4, the spacing between peaks of common *z*-height defines an average terrace height of ~34 Å, consistent with the layer *d*-spacing from specular XRD. The increase in lateral size after heating to a high-temperature phase does not cause an observable change in the specular XRD pattern.

GIXD is used to characterize the in-plane molecular packing, which is highly relevant to the two-dimensional carrier transport that occurs in transistors. Because the GIXD pattern includes out-of-plane contributions, completely indexing the pattern can also permit the determination of a thin-film unit cell.[10,11] The GIXD pattern of a **TQPP-12** film with M1 thermal history is shown in Figure 5. The layer spacing in the GIXD pattern is represented by a series of (00*l*) peaks along the out-of-plane axis (q_z), and corresponds to 34.2 Å, which is consistent with the layer *d*-spacing from specular XRD. The GIXD patterns were similar for AC and M2 thermal histories. The GIXD pattern clearly shows the same large variations with intensity as a function of peak order as observed in the specular diffraction. The complex structure factor is also manifested in the intensity fluctuations of the nonequatorial mixed index peaks. This strong dependence of peak intensity on peak order makes uniquely indexing the unit cell nontrivial, because multiple triclinic cells with varying cell volume, lattice constant, and unit cell angles can reasonably fit the peak locations. Structure factor modeling is required to determine which of these cells is correct, but such modeling is generally intractable for functionalized molecules with significant conformational freedom, such as **TQPP-12**. Important spacing information, however, can be gained by analyzing the GIXD pattern. In Figure 5 we note a prominent in-plane spacing of 9.9 Å that corresponds to the first set of nonequatorial peaks (labeled b); this spacing is similar to the estimated short core axis length of 9.13 Å (AM1) as drawn in Figure 1b and is likely the 01L series. We also note three series of nonequatorial peaks (labeled a_1 to a_3 with spacings of 4.9, 5.1, and 5.4 Å), which closely correspond to the intermolecular spacing expected for cofacial in-plane packing. The series labeled a_2 is most likely the 02L series. The remaining series (a_1 and a_3) are likely the 10L or 11L series, but without a structure factor model, we are unable to make a verifiably unique assignment. Determination of the **TQPP-12** packing style within the unit cell requires additional orientation information, especially with respect to the conjugated core of **TQPP-12**.

NEXAFS spectroscopy[19] can be employed to characterize orientation in films of polymer[6,17] and small molecule[6,18] organic semiconductors. For planar conjugated molecules such as **TQPP-12**, the transition dipole for the 1s $\rightarrow \pi^*$ is perpendicular to the aromatic plane.[19] Figure 6 shows the incident angle dependent carbon K-edge NEXAFS spectra for an AC film. The NEXAFS spectra of the M1 and M2 films (not shown) produced similar results. The angle dependence of the π^* resonance intensity can be expressed as a dichroic ratio, *R*, which can vary from +0.7 for a vertical plane (transition dipole parallel to surface plane) to −1.0 for a horizontal or flat plane (transition dipole parallel to surface normal).[6] An isotropic distribution of planes results in $R = 0$. Analysis of the π^* resonance near 285.5 eV results

(9) Snyder, R. L.; Fiala, J.; Bunge, H. J. *Defect and Microstructure Analysis by Diffraction*; Oxford University Press: Oxford, 1999.
(10) Merlo, J. A.; Newman, C. R.; Gerlach, C. P.; Kelley, T. W.; Muyres, D. V.; Fritz, S. E.; Toney, M. F.; Frisbie, C. D. *J. Am. Chem. Soc.* **2005**, *127*, 3997–4009.
(11) Equation S1 from Supporting Information of ref 10 published as $q_{xy}^2 = h^2(a_{||}^*)^2 + k^2(b_{||}^*)^2 - 2hk\cos(\gamma_{||}^*)$ requires correction and should be used in the form of $q_{xy}^2 = h^2(a_{||}^*)^2 + k^2(b_{||}^*)^2 - 2hk(a_{||}^*)(b_{||}^*)\cos(\gamma_{||}^*)$.
(12) Holmes, D.; Kumaraswamy, S.; Matzger, A. J.; Vollhardy, K. P. C. *Chem.—Eur. J.* **1999**, *5*, 3399–3412.
(13) Mattheus, C. C.; Dros, A. B.; Baas, J.; Meetsma, A.; Boer, J. L. d. B.; Palstra, T. T. M. *Acta Crystallogr., Sect. C: Cryst. Struct. Commun.* **2001**, *C57*, 939–941.
(14) Brédas, J. L.; Calbert, J. P.; da Silva Filho, D. A.; Cornil, J. *Proc. Natl. Acad. Sci. U.S.A.* **2002**, *99*, 5804–5809.
(15) Percec, V.; Glodde, M.; Bera, T. K.; Miura, Y.; Shiyanovskaya, I.; Singer, K. D.; Balagurusamy, V. S. K.; Heiney, P. A.; Schnell, I.; Rapp, A.; Spiess, H. W.; Hudson, S. D.; Duan, H. *Nature* **2002**, *417*, 384.
(16) Schmidt-Mende, L.; Fechtenkotter, A.; Müllen, K.; Moons, E.; Friend, R. H.; MacKenzie, J. D. *Science* **2001**, *293*, 1119–1122.
(17) DeLongchamp, D. M.; Kline, R. J.; Lin, E. K.; Fischer, D. A.; Richter, L. J.; Lucas, L. A.; McCulloch, I.; Heeney, M.; Nortrup, R. *Adv. Mater.* **2007**, *19*, 833–837.
(18) Kafer, D.; Ruppel, L.; Witte, G.; Ch, W. *Phys. Rev. Lett.* **2005**, *95*, 166602.
(19) Stohr, J. *Nexafs Spectroscopy*; Springer: New York, 1996.

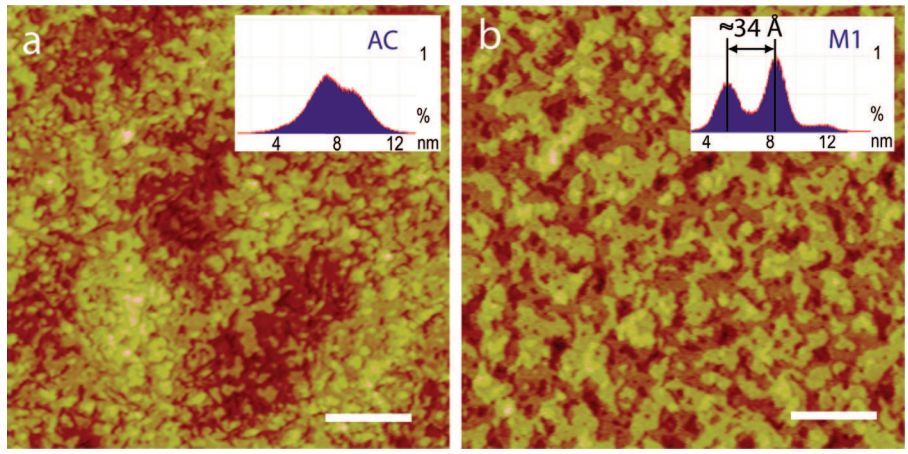

Figure 4. AFM height micrographs of (a) AC and (b) M1 thin films on OTS-modified substrates. For all micrographs, vertical scale is 20 nm and scale bar is equal to 1 μm. Depth profile analysis of each micrograph is used to estimate the terrace height (see Supporting Information). M1 shows terrace formation of ≈34 Å in height upon heating. M2 produced similar AFM results (not shown) to M1.

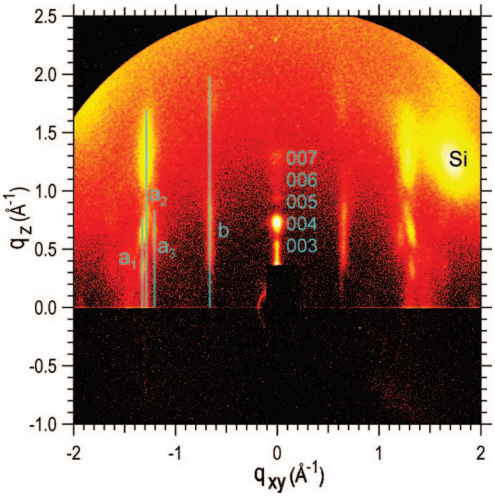

Figure 5. GIXD of M1 film. The primary out-of-plane (001) reflection is blocked by the beam stop of the instrument. GIXD of AC and M2 film (not shown) produced similar results.

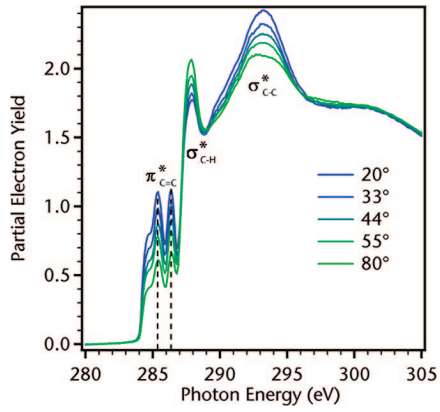

Figure 6. NEXAFS spectrum of AC film. NEXAFS spectra of M1 and M2 films (not shown) shows similar results.

in $R = -0.36 \pm 0.01$ and -0.39 ± 0.02, respectively, for AC and M1, indicating a mild plane-on preference. The broad carbon−carbon 1s → σ^* resonance near 293 eV is dominated by contributions from the dodecyl chains, with minor contributions from the conjugated core. Assuming the 1s → σ^* transition dipole lies along the average side-chain director,[20] the dichroic ratio will vary from +0.7 for a horizontal chain to −1.0 for a vertical chain. The side-chain dichroic ratios for films on OTS-modified Si were $R = -0.15 \pm 0.02$, indicating a slight vertical preference compared to the disorder condition. Similar values were obtained for the M1 and M2 thermal histories, consistent with specular XRD, which indicated that the layer structure was similarly unaffected.

NEXAFS spectroscopy in partial electron yield mode is surface sensitive, with most of the signal dominated by the uppermost ~4 nm of the film. It therefore is necessary to evaluate whether molecular orientation is comprehensive throughout the film. Using a film delamination technique,[17,21] NEXAFS spectroscopy can be used to probe the **TQPP-12** at the OTS interface. We find that conjugated plane and side-chain orientations of the bottom interface are, within uncertainty, identical to those measured on the top surface, indicating that a consistent molecular orientation persists throughout the film thickness. This result is consistent with the specular XRD, which indicated that a single layer type persists throughout the film.

On the basis of the high levels of order and orientation determined by XRD, the comprehensive terracing observed in AFM, and the confirmation by delamination NEXAFS spectroscopy that molecular orientation is constant throughout the film, it is reasonable to assume comprehensive crystallinity of a single type with a common orientation relative to the substrate. It is further reasonable to assume a monomolecular basis and a monomodal molecular orientation distribution, which we will further justify below. On the basis of these assumptions, we can interpret the R values determined by NEXAFS as specific tilts for the conjugated plane normal and the side chains. The average conjugated plane tilt from the surface normal is determined by NEXAFS is ~48°. Accounting for the contribution to the 1s → σ^* feature due to the core, as

(20) Hahner, G.; Kinzler, M.; Woll, C.; Grunze, M.; Scheller, M. K.; Cederbaum, L. S. *Phys. Rev. Lett.* **1991**, *67*, 851.
(21) Chabinyc, M. L.; Salleo, A.; Wu, Y. L.; Liu, P.; Ong, B. S.; Heeney, M.; McCulloch, L. *J. Am. Chem. Soc.* **2004**, *126*, 13928–13929.

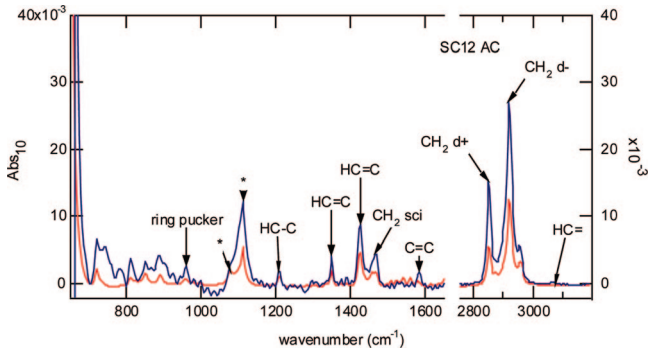

Figure 7. FTIR s-polarized (blue) and p-polarized (red) spectra for AC. The IR spectra of the M1 and M2 films (not shown) produced similar results. Principle lines used in analysis are labeled. Features marked with * are corrupted by miscancelation of SiO features (from both oxide and bulk impurities).

Table 1. IR Vibrational Resonances and Assignments for TQPP-12 and Calculated Dichroism Ratio (A_p/A_s)

wavenumber (cm^{-1})	assignment	A_p/A_s	note
3068	H−C	0.04	core *y*
2920	antisymmetric CH_2	0.46	chain *y*
2851	symmetric CH_2	0.35	chain *x*
1584	C=C	0.11	core *y*
1464	scissor	0.41	chain *x*
1426	HC=C	0.52	core *z*
1349	HC=C	0.51	core *z*
1209	HC-C	0.58	core *z*
1081	C−C	0.60	core *z*
957	ring pucker	0.19	core *y*

described in the Supporting Information, the side-chain tilt from the surface normal is ∼45°.

Molecular orientation can be further elaborated by polarized IR spectroscopy, which is sensitive to the orientation of the vibrationally distinct chemical functional groups in a molecule. Shown in Figure 7 are the p- and s-Brewster's angle polarized absorption spectra for the AC film. The IR spectra of the M1 and M2 films (not shown) showed similar features. The primary features were assigned based on comparison to quantum chemical calculations (see the Supporting Information) and are summarized in Table 1. Resonances useful in characterization of the **TQPP-12** core are primarily within the 950−1450 cm^{-1} region while the CH stretching features of the alkyl side chains dominate the (2800−2930 cm^{-1}) region. The core is of D_{2h} symmetry and all IR modes lie along one of the three C_2 axes. The transition dipole orientation is also given in Table 1 with *x*,*y*,*z* as defined in Figure 1b. The dichroism of the vibrational resonances is characterized by the ratio of the *p*- versus *s*-polarized absorption A_p/A_s. The average A_p/A_s values for the principal features are also given in Table 1. From the A_p/A_s values, one can calculate the average tilt of the respective director from the surface normal, assuming a tight monomodal orientation distribution as in the NEXAFS analysis.[8] The calculation requires both the film thickness and the nonresonant index of refraction. The film thickness was taken from visible ellipsometry, while IR ellipsometry measurements were used to determine the index of refraction in the mid-IR: 1.62. The derived director tilts are summarized in Table 2. The short axis of the core

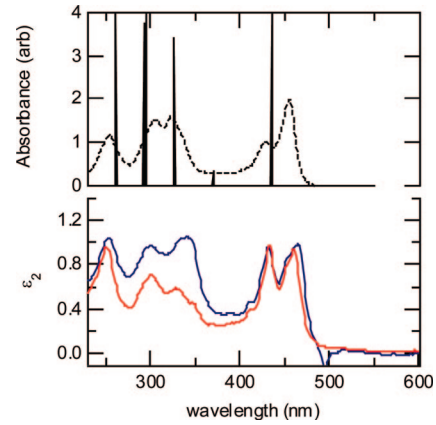

Figure 8. Upper: **TQPP-12** solution absorption spectrum (dashed) and ZINDO/S calculation (solid). Lower: From SE, imaginary part of in-plane (blue) and out-of-plane (red) film dielectric function.

Table 2. TQPP-12 Net Orientations Measured From Surface Normal

	NEXAFS, deg	IR, deg
core *z*		51 ± 2
core *y*		81 ± 8
core π	∼48	41 ± 2
chain *x*		59 ± 1
chain *y*		54 ± 1
chain *z*	∼45°	51 ± 2

(core *y*) lies essentially in the surface plane, while the long axis (core *z*) is significantly tilted from surface normal. The measured orientation of the short axis of the core is incompatible with a herringbone packing arrangement, and therefore supports our assumption of a monomolecular basis. On the basis of the assumption of orthogonality, one can also calculate the π director tilt for direct comparison with the NEXAFS results. This comparison is summarized in Table 2. The two techniques are in remarkably good agreement.

IR spectroscopy can also be used to determine the configuration and orientation of the dodecyl side chains. The position of the methylene antisymmetric stretch (ν_aCH_2) is a qualitative diagnostic for chain order. Crystalline all-trans systems exhibit $\nu_aCH_2 \approx 2918$ cm^{-1}, whereas $\nu_aCH_2 \approx 2928$ cm^{-1} for liquid alkanes.[22,23] For **TQPP-12**, $\nu_aCH_2 = 2919.7$ cm^{-1} for both AC and M1 thermal histories, indicating highly ordered side chains. The side-chain angle derived from the mutually orthogonal symmetric and asymmetric stretches of the CH_2 is 51 ± 2°, again consistent with the NEXAFS determination (see Table 2).

Shown in Figure 8 is the dilute solution UV−vis absorption spectrum of **TQPP-12** in dichloromethane and the principal predicted singlet transitions from a ZINDO/S calculation. The calculation was performed in Gaussian03[24] using the ground-state structure determined by density functional theory using the B3LYP functional[25] and a 6−31/G** basis set. All of the transitions are polarized along the core *z*-axis except for the 293 nm

(22) Snyder, R. G.; Maroncelli, M.; Strauss, H. L.; Hallmark, V. M. *J. Phys. Chem.* **1986**, *90*, 5623–5630.
(23) Snyder, R. G.; Strauss, H. L.; Elliger, C. A. *J. Phys. Chem.* **1982**, *86*, 5145–5150.

component of the doublet near 290 nm and the weak absorption at 370 nm, which are polarized along the core short axis. The first $B_{1u} \leftarrow A_g$ transition near 450 nm has significant vibronic structure, consistent with coupling to a $\approx$1300 cm^{-1} core skeletal vibration. Also shown in Figure 8 is the imaginary part of the uniaxial thin film dielectric function, as determined by SE. There is a slight red shift, from 455 to 466 nm of the 0−0 transition of the film with respect to the solution. The dichroism of the film can be quantitatively related to the orientation of molecule via the known orientation of the transition dipoles. Transition dipoles with tilts from the surface normal near the magic angle: 54.7° result in an isotropic absorption. The film is not strongly dichroic, qualitatively consistent with the NEXAFS and IR results. The mixed polarization of the transitions near 300 nm prohibit a quantitative orientation analysis. The presence of coupled, translationally inequivalent molecules in a crystal leads to Davydov splitting of the absorption features.[26] This is not clearly present for **TQPP-12**; however, there is a significant redistribution of intensity between the 0−0 and 0−1 vibronic components of the thin film spectrum with respect to the solution case, suggesting changes in the localization of the excited state in the solid. Similar changes in vibronic coupling have been observed for perylene diimide chromophores and are attributed to the formation of cofacial dimers (strong 0−1 transition) vs monomers (strong 0−0 transition).[27] Thus the absorption spectrum suggests significant interactions between near equivalent molecules for **TQPP-12**.

The molecular spectroscopies, NEXAFS, SE, and FTIR, allow the orientations of all parts of **TQPP-12** to be described as shown in Figure 9a. The short axis is parallel to the substrate plane. The long axis of the core is tilted and the side chains are slightly tilted from the core. We have assumed for this illustration that the side chains are azimuthally rotated such that they are roughly aligned to the core long axis, although any azimuthal rotation is possible. The molecule as shown in Figure 9a would have a vertical height of 33.4 which is consistent with the layer spacing determined via

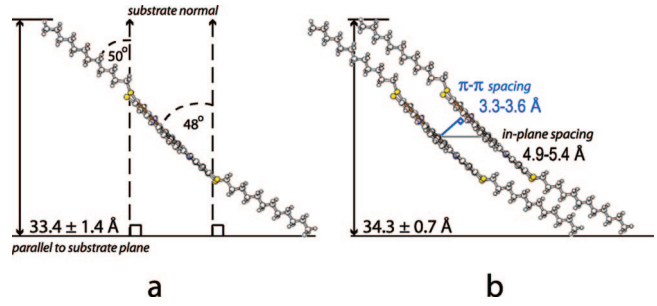

Figure 9. Proposed molecular packing style of **TQPP-12.** (a) Molecular orientation as determined from spectroscopies. The relative azimuthal rotation between the side chains and the backbone is unknown. (b) **TQPP-12** lattice viewed along the molecular short axis according to spacings determined from XRD and GIXD. In-plane spacing approximately the length of the short axis was also observed. Standard uncertainty in lattice parameters is 2%.

XRD ((34.3 ± 0.3) Å). These results indicate that there is no interdigitation of alkane side chains between adjacent layers. The lack of interdigitation is further supported by the closest-packed side-chain density for **TQPP-12**, which can be calculated by determining the in-plane side-chain attachment density enforced by core packing and then finding the spacing between chains at a given chain tilt. The closest-packed side-chain density of **TQPP-12** is comparable to that of crystalline polyethylene (5.6×10^{14} methylenes/cm^2 for **TQPP-12** vs 5.4×10^{14} methylenes/cm^2 for polyethylene), leaving no room for side-chain interdigitation (see the Supporting Information for more details on the side-chain density calculation).[28] Given the proposed core orientation, a herringbone packing of the cores is forbidden because two adjacent molecules with the same long axis tilt cannot engage in a close edge-to-face interaction without substantially tilting the short axis out-of-plane. This conclusion is supported by the suggestion of cofacial packing from the absorption spectrum.

The proposed molecular packing style determined from the spectroscopic orientation information is in agreement with the layer spacing determined by GIXD. Figure 9b shows the packing of **TQPP-12**, projected along the *b*-axis. We have assumed for this illustration that the core long axis tilts in the same direction as β. The refinement in core tilt allows us to calculate the $\pi-\pi$ interplane stacking distance, as shown in Figure 9b. Using the GIXD in-plane spacing and the conjugated plane tilt determined by NEXAFS, the $\pi-\pi$ stacking distance is in the range of 3.3−3.6 Å, in excellent agreement with commonly reported values.[14–16]

Conclusions

The thin film microstructure of the complex organic semiconductor **TQPP-12** was characterized by complementing lattice information from XRD with orientation information from the polarized photon absorption spectroscopies FTIR, SE, and

(24) Gaussian 03, R. C., Frisch, M. J.; Trucks, G. W.; Schlegel, H. B.; Scuseria, G. E.; Robb, M. A.; Cheeseman, J. R.; Montgomery, J. A., Jr.; Vreven, T.; Kudin, K. N.; Burant, J. C.; Millam, J. M.; Iyengar, S. S.; Tomasi, J.; Barone, V.; Mennucci, B.; Cossi, M.; Scalmani, G.; Rega, N.; Petersson, G. A.; Nakatsuji, H.; Hada, M.; Ehara, M.; Toyota, K.; Fukuda, R.; Hasegawa, J.; Ishida, M.; Nakajima, T.; Honda, Y.; Kitao, O.; Nakai, H.; Klene, M.; Li, X.; Knox, J. E.; Hratchian, H. P.; Cross, J. B.; Bakken, V.; Adamo, C.; Jaramillo, J.; Gomperts, R.; Stratmann, R. E.; Yazyev, O.; Austin, A. J.; Cammi, R.; Pomelli, C.; Ochterski, J. W.; Ayala, P. Y.; Morokuma, K.; Voth, G. A.; Salvador, P.; Dannenberg, J. J.; Zakrzewski, V. G.; Dapprich, S.; Daniels, A. D.; Strain, M. C.; Farkas, O.; Malick, D. K.; Rabuck, A. D.; Raghavachari, K.; Foresman, J. B.; Ortiz, J. V.; Cui, Q.; Baboul, A. G.; Clifford, S.; Cioslowski, J.; Stefanov, B. B.; Liu, G.; Liashenko, A.; Piskorz, P.; Komaromi, I.; Martin, R. L.; Fox, D. J.; Keith, T.; Al-Laham, M. A.; Peng, C. Y.; Nanayakkara, A.; Challacombe, M.; Gill, P. M. W.; Johnson, B.; Chen, W.; Wong, M. W.; Gonzalez, C.; Pople, J. A.; Gaussian, Inc., Wallingford, CT, 2004.
(25) Becke, A. D. J. *Chem. Phys.* **1993**, *98*, 5648–5652.
(26) Davydov, A. S. *Theory of Molecular Excitons*; Plenum: New York, 1971.
(27) Li, A. D. Q.; Wang, W.; Wang, L.-Q. *Chem.—Eur. J.* **2003**, *9*, 4594–4601.
(28) Kline, R. J.; DeLongchamp, D. M.; Fischer, D. A.; Lin, E. K.; Richter, L. J.; Chabinyc, M. L.; Toney, M. F.; Heeney, M.; McCulloch, I. *Macromolecules* **2007**, *40*, 7960–7965.

NEXAFS. Despite the observed phase transitions in powder DSC, thermal history had a minimal effect on the thin film microstructure. The characterization strategy proved effective at determining a nearly complete crystal packing model. Notable features of the packing are the arrangement in segregated vertical layers, the highly tilted core long axes and side chains within the layers, the absence of alkane interdigitation between layers, and the cofacial packing of tilted planes. Future studies will develop deeper correlations between primary chemical structure, crystal structure, and carrier mobility by determining how crystal structure and mobility vary with changing alkane side-chain length.

Acknowledgment. L.A.L. thanks the Alcatel-Lucent Bell Labs Graduate Research Fellowship and mentor Alice White. The work at the American University of Beirut (AUB) was supported by the University Research Board (URB) and the Lebanese National Council for Scientific research (LNCSR). B.R.K. thanks AUB for a faculty development fund.

Supporting Information Available: Density functional theory quantum chemical calculations performed with the Gaussian03 program used to assign the vibrational spectra, along with details of the NEXAFS analysis (PDF). This material is available free of charge via the Internet at http://pubs.acs.org.

CM702802W